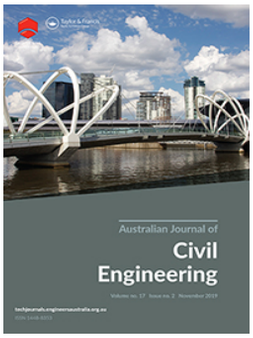

Taylor & Francis
Taylor & Francis Group

Australian Journal of Civil Engineering

ISSN: 1448-8353 (Print) 2204-2245 (Online) Journal homepage: https://www.tandfonline.com/loi/tcen20

Two dimensional bed deformation model in turbulent streams

Amin Gharehbaghi, Birol Kaya & Gökmen Tayfur

To cite this article: Amin Gharehbaghi, Birol Kaya & Gökmen Tayfur (2019) Two dimensional bed deformation model in turbulent streams, Australian Journal of Civil Engineering, 17:2, 73-84, DOI: 10.1080/14488353.2019.1618628

To link to this article: https://doi.org/10.1080/14488353.2019.1618628

AUSTRALIAN JOURNAL OF CIVIL ENGINEERING
2019, VOL. 17, NO. 2, 73–84
https://doi.org/10.1080/14488353.2019.1618628

Taylor & Francis
Taylor & Francis Group

ARTICLE

Two dimensional bed deformation model in turbulent streams

Amin Gharehbaghi[a], Birol Kaya[a] and Gökmen Tayfur[b]

[a]Civil Engineering Department, DokuzEylül University, Izmir, Turkey; [b]Civil Engineering Department, Izmir Institute of Technology, Izmir, Turkey

ABSTRACT

A coupled model is developed to simulate two dimensional water surface profile, suspended sediment load and bed deformation in unsteady open channels. The hydrodynamical component employs the two dimensional shallow water equations to obtain the hydraulic variables. These, in turn, are used in the morphdynamical component to determine the bed deformation. For the turbulence variables; two turbulence models are supervened to the governing equations. Triangular meshes were developed to discretize the domain of open channel. In order to discretize the governing equations, the explicit finite volume method is used by the total variation diminishing (TVD) schemes. The performance of the developed model is compared to that of the Flow3D software. The comparison results are in good agreement.

ARTICLE HISTORY
Received 21 November 2017
Accepted 7 May 2019

KEYWORDS
Finite volume method; turbulence model; total variation diminishing (TVD) schemes; two dimensional unsteady flow; shallow water equations; unstructured grid system

1. Introduction

To simulate the water surface profiles and bed deformations, researchers employed the Navier–Stokes equations (NSE) or the simplified version of NSE, which are the shallow water equations (SWE). In many of works, researchers preferred to simulate bed deformations in One dimensional (1D) condition (Gharehbaghi and Kaya 2011; Kaya and Gharehbaghi 2012; Seo, Jun, and Choi 2009; Tayfur and Singh 2006; Tayfur and Singh 2007; V´azquez-Cend´on, Cea, and Puertas 2009; Wu, Vieira, and Wang 2004, among many). Because of complexity in most of the models, scientists have usually ignored the turbulence models that can play key roles in the simulation of flow in turbulent conditions.

Various numerical techniques are developed by scientists to handle the computational fluid dynamic (CFD) problems. Finite Difference Method (FDM), Finite Element Method (FEM) and Finite Volume Method (FVM) are popular in this domain. One of the key steps in the numerical solutions is the meshing step. In irregular and curvilinear geometry, developing unstructured mesh is necessary. Applying an unstructured mesh to FDM is not easy. Moreover, FDM in the same size of mesh and time steps can produce less sensitive results than FEM or FVM (Kaya and Gharehbaghi 2014). FEM could discretize the complex geometry. However, applying FEM is more difficult than the FVM. Moreover, FVM could keep the balance of the amount of mass and momentum by solving the integral form of the conservation equations (Gharehbaghi, Kaya, and Saadatnejadgharahassanlou 2017). FVM does not require a continuous form of computational domain (Gharehbaghi, Kaya, and Saadatnejadgharahassanlou 2017).

Farsirotou, Soulis, and Dermissis (2002) proposed a Two Dimensional (2D) numerical model that could determine bed deformation in alluvial channels in sub and/or supercritical conditions. In their work, an explicit FVM was employed to discretize the coupled model of vertically averaged free-surface flow equations and sediment transport equation. Liu, Landry, and García (2008), by solving SWE and sediment transport equations, tried to simulate 2D bed variation. In their model, FVM, by Godunov's scheme on unstructured mesh system, was applied to solve the governing equations. Furthermore, Roe's approximate Riemann solver was used to determine the inviscid fluxes. In their work, they enforced the extrapolation method of the TVD scheme for the upwind ratio of consecutive gradients that were based on the virtual upwind node.

Castro Diaz et al. (2009), in order to simulate water surface profile and sediment transport phenomenon, proposed a 2D model. SWE and sediment transport discharge formula were used to calculate the hydrodynamic and morphodynamic components, respectively. For the sake of discretizing the governing equations; in the first step, they considered a Roe-type first order scheme as well as a variant based one on the use of flux limiters. In the second step, these first-order schemes were extended to second-order accuracy by means of a novel MUSCL-type reconstruction operator on unstructured meshes. In fact,

CONTACT Amin Gharehbaghi gharehbaghi.amin@gmail.com Civil Engineering Department, DokuzEylül University, Tinaztepe Campus, Izmir 35160, Turkey

they enforced a second order MUSCL reconstruction operator in space and a second order TVD Runge-Kutta method. Amoudry and Liu (2009) presented a model that could calculate two-dimensional, two-phase, and non-cohesive sediment transport. In their model, they applied concentration-weighted averaged equations of motion for both fluid and sediment phases. Moreover, a collisional theory was used to determine the sediment stresses, while modified k–ε turbulence model was employed. Kuang et al. (2011) presented semi-implicit Eulerian–Lagrangian method, unstructured SWAN model, CurWaC2D-Sed and FVM to develop 2D morphological model. Cea and Vázquez-Cendón (2012) presented a novel unstructured upwind FVM for discretization of the bed friction term. Gharehbaghi, Kaya, and Saadatnejadgharahassanlou (2017) established a new depth-averaged 2D non-equilibrium coupled model. This model can calculate water surface profiles and bed profiles in alluvial channels and rivers. In this research, they used two turbulence models for examining the turbulence parameters.

In recent years, many researchers tried to apply turbulence models in sediment transport phenomenon in open channels and rivers. Therefore, various kinds of turbulence models have been developed. Yafei and Wang (2001) developed 2D hydrodynamic and sediment transport model for unsteady open channel flows based on the FEM that is called CCHE2D. In this model they implemented the depth averaged parabolic Eddy viscosity model, the mixing length model and the depth-integrated k-ε model. Barrios-Piña et al. (2014) introduced Three Dimensional (3D) model that focused on the effects of vegetation on a fluid flow pattern. In their work, they applied the horizontal mixing-length in explicit conditions and they coupled it with the multi-layer approach for the vertical mixing-length within a general 3D Eddy-viscosity formulation.

In recent years, due to its advantages, TVD scheme has become more popular in open channel flows and rivers. The basic upwind differencing scheme introduces a high level of false diffusion due to its low order of accuracy (first-order) (Versteeg and Malalasekera 2007). 'Higher-order schemes such as central differencing and Quadratic upwind differencing (QUICK) can give spurious oscillations or 'wiggles' when the Peclet number is high. When such higher-order schemes are used to solve turbulent quantities, turbulence energy and rate of dissipation, wiggles can give physically unrealistic negative values and instability. TVD schemes are designed to address this undesirable oscillatory behaviour of higher-order schemes. In TVD schemes, the tendency towards oscillation is counteracted by adding an artificial diffusion fragment or by adding a weighting towards upstream contribution' (Versteeg and Malalasekera 2007). García-Navarro, Alcrudo, and Savirón (1992) introduced an addition of a dissipation step to the McCormack numerical scheme for solving 1D open-channel flow equations. This extra step is devised according to the theory of TVD schemes. They presented results from several computations and compared the results with the analytical solutions for some test problems. As presented in Castro Diaz et al. (2009), TVD scheme was applied in 2D model to determine water surface profile and sediment transport phenomenon. However, they did not consider any turbulence models. Liu, Landry, and García (2008) used the extrapolation method of the TVD scheme for the upwind ratio of consecutive gradients. Researchers have preferred to apply TVD scheme by Riemann solver. In this study however it is preferred to use TVD approximation directly. The codes are developed in MATLAB. One of the novel contributions of this paper is that TVD scheme has been directly employed in the simulation of two dimensional bed deformation and suspended sediment load by two simple but useful turbulence models.

The main goal of this work is to develop 2D model to determine water surface profile and bed deformation in unsteady open channels. Most of the developed models in this field have ignored the turbulent models. In this study, two turbulent models (Depth averaged parabolic eddy viscosity turbulence model and mixing length turbulence model) are employed. As stated previously, the authors of this paper in 2017 proposed a numerical model in this field. The mentioned model calculated the problems in non-equilibrium conditions. Nevertheless, the overwhelming majority of the researchers prefers to solve the problems in equilibrium conditions. Thus, in this study we decided to modify the developed model, and solve the problems in equilibrium conditions. One of the advantages of the established model is that it could perform the computations with a coarser mesh than the Flow3D software and satisfies the required accuracy. The developed model in this study is a coupled model that has the combination of hydrodynamical and morphodynamical components. Two dimensional SWE and empirical relations of sediment transport phenomenon are employed. The model is tested against the Flow3D software which is commonly employed in experimental and numerical studies (Acharya 2011; Afshar and Hoseini 2013; Vasquez, Hurtig, and Hughes 2013; Vasquez and Walsh 2009, among many).

2. Governing equations

The general form of 2D SWE for simulation of water surface profile and bed variation in Cartesian coordinates could be found in several studies (V´azquez-Cend´on, Cea, and Puertas 2009; Yulistiyanto 2009, among many):

$$\frac{\partial Q}{\partial t}+\frac{\partial F_x}{\partial x}+\frac{\partial F_y}{\partial y}=S \tag{1}$$

$$Q=\begin{bmatrix} h \\ hu \\ hv \\ z \end{bmatrix} \tag{2}$$

$$F_{\mathrm{x}}=\begin{bmatrix} hu \\ \frac{1}{2}gh^2+hu^2-\frac{h}{\rho_w}T_{xx} \\ huv-\frac{h}{\rho_w}T_{yx} \\ \varepsilon q_{b,x} \end{bmatrix} \tag{3}$$

$$F_{\mathrm{y}}=\begin{bmatrix} hv \\ huv-\frac{h}{\rho_w}T_{xy} \\ \frac{1}{2}gh^2+hv^2-\frac{h}{\rho_w}T_{yy} \\ \varepsilon q_{b,y} \end{bmatrix} \tag{4}$$

$$S=\begin{bmatrix} 0 \\ gh\left(\frac{\partial z}{\partial x}+s_{0x}\right)-s_{fx}-\frac{\tau_{bx}}{\rho_w} \\ gh\left(\frac{\partial z}{\partial y}+s_{0y}\right)-s_{fy}-\frac{\tau_{by}}{\rho_w} \\ 0 \end{bmatrix} \tag{5}$$

$$\begin{cases} S_{0x}=\frac{\partial \bar{H}}{\partial x} \\ S_{0y}=\frac{\partial \bar{H}}{\partial y} \end{cases} \tag{6a, b}$$

$$\varepsilon=\frac{1}{1-P} \tag{7}$$

$$\bar{H}=H-z \tag{8}$$

where; Q is the conserved vector (the time derivative of the components); F_x and F_y are derivation of the components in the x- and y-directions, respectively and S is the source term. g is the gravity acceleration; h is the depth of water; z is the thickness of the sediment layer (see Figure 1); ρ_w is the flow density; P is the sediment porosity; u and v are the components of the depth averaged velocity in the x- and y-directions, respectively. $S_{0,x}$, $S_{0,y}$ are the bed slopes and, $S_{f,x}$, $S_{f,y}$ are the friction slopes in the x- and y-directions, respectively. $q_{b,x}$ and $q_{b,y}$ are the sediment transport discharge in the movable bed layer in x- and y- direction, respectively. τ_{bx} and τ_{by} are the bed shear stress in x- and y-direction, respectively and T_{xx}, T_{xy}, T_{yx}, T_{yy} are the depth averaged turbulence stresses. $\bar{H}$ is the difference between non-erodible bottom and reference level, and H is the difference between erodible bottom and reference level (see Figure 1).

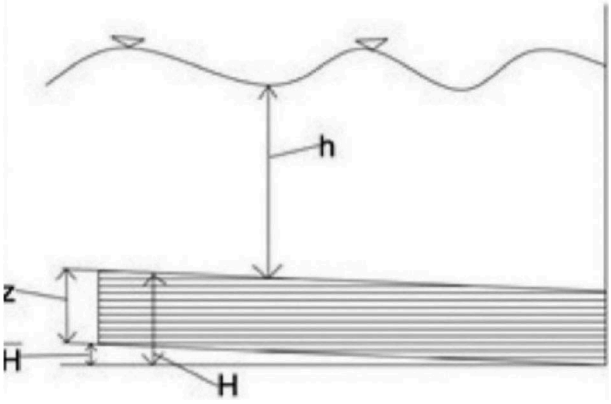

Figure 1. Illustration of sediment layer in an open channel (Gharehbaghi, Kaya, and Saadatnejadgharahassanlou 2017).

τ_{bx} and τ_{by} are expressed as follows (Wu, Vieira, and Wang 2004):

$$\begin{cases} \tau_{bx}=\rho_w.c_f.u\sqrt{u^2+v^2} \\ \tau_{by}=\rho_w.c_f.v\sqrt{u^2+v^2} \end{cases} \tag{9a, b}$$

$$c_f=gn^2\Big/h^{1}/_{3} \tag{10}$$

The Boussinesq's assumptions for turbulent stresses are given as:

$$\begin{cases} T_{xx}=2\rho_w(\nu+\nu_t)\frac{\partial u}{\partial x}-\frac{2}{3}\rho_w k \\ T_{xy}=T_{yx}=\rho_w(\nu+\nu_t)\left(\frac{\partial u}{\partial y}+\frac{\partial v}{\partial x}\right) \\ T_{yy}=2\rho_w(\nu+\nu_t)\frac{\partial v}{\partial y}-\frac{2}{3}\rho_w k \end{cases} \tag{11a, b, c}$$

where; ν and ν_t are the kinematic and Eddy viscosity of water, respectively and k is the turbulence energy. When considering zero-equation turbulence models, this term can be ignored. Meyer-Peter and Muller (1948) presented experimental relations to determined sediment flux in open channels and rivers. In this study, this relation was selected to determine the solid transport discharge and Chien (1956) proved that the original formula can be reduced to the following expression,

$$\begin{cases} q_{b,\mathrm{x}}=8\sqrt{(G-1)gd_i^3}\,\frac{u}{\sqrt{u^2+v^2}}\,max\left(\tau_*-\tau_{*,c},0\right)^{3/2} \\ q_{b,\mathrm{y}}=8\sqrt{(G-1)gd_i^3}\,\frac{v}{\sqrt{u^2+v^2}}\,max\left(\tau_*-\tau_{*,c},0\right)^{3/2} \end{cases} \tag{12a, b}$$

$$\tau_*=\frac{\gamma_w n^2(u^2+v^2)^{3/2}}{(P_s-P)d_i h^{1/3}} \tag{13}$$

$$\begin{cases} S_{f,\mathrm{x}}=\frac{n^2u\sqrt{u^2+v^2}}{h^{4/3}} \\ S_{f,\mathrm{y}}=\frac{n^2v\sqrt{u^2+v^2}}{h^{4/3}} \end{cases} \tag{14a, b}$$

where; τ_* and $\tau_{*,c}$ are the shear stress and critical bed shear stresses in sediment transport phenomenon, respectively; d_i is the size of bed materials; ρ_w is the density of flow; n is the Manning coefficient; γ_w is the specific weight of the fluid and G is the proportional density that equal to density of sediment to density of water.

3. Turbulence models

3.1. Depth-averaged parabolic eddy viscosity model

Depth averaged parabolic eddy viscosity model can be obtained by averaging the eddy viscosity, which approximately yields a parabolic profile, over the flow depth. The equations of depth-averaged parabolic eddy viscosity model are given in Wu, Vieira, and Wang (2004) as follows.

$$v_t = \propto_t u_* h \tag{15}$$

where u_* is the bed shear velocity and $\propto_t$ is an empirical coefficient.

$$\propto_t = \frac{v_k}{6} \tag{16}$$

$$u_* = \left[c_f\left(u^2 + v^2\right)^2\right]^{1/2} \tag{17}$$

where v_k is the van Karman's constant (v_k = 0.41). As noted before by considering zero-equation turbulence models, turbulence energy parameter can be ignored.

3.2. Mixing length model

Depth averaged parabolic eddy viscosity model is the simple turbulence model. This model is applicable in the region of main flow, but it does not account for the influence of the horizontal gradient of velocity. Significant errors may exist when it is applied in the region close to rigid walls (Wu, Vieira, and Wang 2004). In order to improve this problem mixing length model can be employed as Yafei and Wang (2001):

$$v_t = l_n^2\sqrt{2\left(\frac{\partial u}{\partial x}\right)^2 + 2\left(\frac{\partial v}{\partial y}\right)^2 + \left(\frac{\partial u}{\partial y} + \frac{\partial v}{\partial x}\right)^2 + \left(\frac{\overline{\partial U}}{\partial z}\right)^2} \tag{18}$$

$$l_n = \frac{1}{h}\int v_k.z\sqrt{\left(1 - \frac{z}{h}\right)}dz = v_k.h\int_0^1 \varsigma\sqrt{(1-\varsigma)}d\varsigma \approx 0.267 v_k.h \tag{19}$$

$$\frac{\overline{\partial U}}{\partial z} = \frac{1}{h}\int\frac{\partial U}{\partial z}dz = \frac{u_*}{v_k.h}\int_{z_0}^{\eta}\frac{1}{z}dz = C_m\frac{u_*}{v_k.h} \tag{20}$$

where l_n is the horizontal mixing length, h is the depth of water, u_* is the bed shear velocity, U is the total velocity. ς is the relative depth of the flow and C_m is a coefficient (2.34,375). The value of turbulence energy is ignored.

4. Discretisation technics by FVM

The main goal of this research is to develop a model to simulate 2D water surface profile and bed deformation in open channels and rivers. One of the key steps in the numerical solution is about the discretization techniques that are applied to the governing equations. In this work; Total Variation Diminishing (TVD) scheme is applied in FVM. By considering the divergence theorem; Equation (1) can be written as:

$$\iint_\Omega \frac{dQ}{dt} + \int_{\partial\Omega} F.ndl = \iint_\Omega SdW \tag{21}$$

where n, dl, dW, Ω, and F are the unit outward vector normal to the boundary elements, sides and areas of triangular meshes, control volume and the vector of normal flux that is equal to $F = [F_x, F_y]^T$, respectively.

If we assume that Q is constant in the centre of each cell, the result of discretisation can be given in basic form as:

$$\mathrm{A}\frac{dQ}{dt} + \sum_{m=1}^{M} F_n^m.L^m = AS \tag{22}$$

where A, m, L^m and $F_n{}^m$ are the area, number of side, length of the m^{th} component and normal of flux to each side of each cells, respectively. The illustration of FVM triangular domain is given in Figure (2).

By considering the angle between x- axis and n direction, which can be called as ($\emptyset$) in counter clockwise, and by applying the rotational invariance to the governing equations the normal of intercell flux for each side of cells is given as:

$$\begin{aligned} F_n(Q) &= F_x\cos\emptyset + F_y\sin\emptyset = T(\emptyset)^{-1}F[T(\emptyset)Q] \\ &= T(\emptyset)^{-1}F\left(\bar{\emptyset}\right) \end{aligned} \tag{23}$$

$$\bar{Q} = \begin{bmatrix} h \\ hu_n \\ hv_n \\ z \end{bmatrix} \tag{24}$$

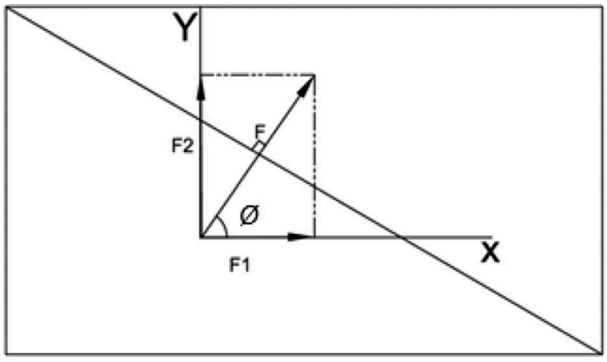

Figure 2. Illustration of FV triangular domain (Gharehbaghi, Kaya, and Saadatnejadgharahassanlou 2017).

$$k_s = \varepsilon.8\sqrt{(G-1)gd_i^3}\,max\left(\tau_* - \tau_{*,c}, 0\right)^{3/2} \quad (25)$$

$$F(\bar{Q}) = \begin{bmatrix} hu_n \\ \frac{1}{2}gh^2 + hu_n{}^2 - \frac{h}{\rho}T_{nn} \\ hu_n v_n - \frac{h}{\rho}T_{nr} \\ \varepsilon k_s \frac{u_n}{\sqrt{u_n^2+v_n^2}} \end{bmatrix} \quad (26)$$

$$T(\emptyset) = \begin{bmatrix} 1000 \\ 0cos\emptyset sin\emptyset 0 \\ 0 - sin\emptyset cos\emptyset 0 \\ 0001 \end{bmatrix} \quad (27)$$

$$T(\emptyset)^{-1} = \begin{bmatrix} 1000 \\ 0cos\emptyset - sin\emptyset 0 \\ 0sin\emptyset cos\emptyset 0 \\ 0001 \end{bmatrix} \quad (28)$$

$$\begin{cases} u_n = ucos\emptyset + vsin\emptyset \\ v_n = vcos\emptyset - usin\emptyset \end{cases} \quad (29)$$

$$\begin{cases} T_{xx} = T_{nn}cos\emptyset \\ T_{yy} = T_{nn}sin\emptyset \\ T_{yx} = T_{nr}sin\emptyset \\ T_{xy} = T_{nr}cos\emptyset \end{cases} \quad (30a, b, c, d)$$

where $F(\bar{Q})$ is the transformed form of normal flux and $T(\emptyset)$ and $T(\emptyset)^{-1}$ are the transformation and inverse transformation matrices, respectively. By applying some substitutions and manipulations on Equation (22), this relation can be rewritten as:

$$A\frac{dQ}{dt} + \sum_{m=1}^{M} T(\emptyset)^{-1}F(\bar{Q})L^m = AS \quad (31)$$

It is worth noting that, in Equation (31), the key point is to develop a method to determine$F(\bar{Q})$.

5. TVD scheme

Considering the illustration of 1D standard control volume in Figure 3, the east face value of upwind differencing (UD) scheme is expressed by the following expression

$$\forall_e = \forall_P \quad (32)$$

The east face value of linear upwind differencing (LUD) scheme is given as:

$$\forall_e = \forall_P + \frac{\delta x}{2}\frac{(\forall_P - \forall_W)}{\delta x} = \forall_P + \frac{1}{2}(\forall_P - \forall_W) \quad (33)$$

The east face value of Quadratic upwind differencing (QUICK) scheme can be written as

$$\begin{aligned} \forall_e &= \frac{6}{8}\forall_P + \frac{3}{8}\forall_E - \frac{1}{8}\forall_W \\ &= \forall_P + \frac{1}{8}(3\forall_E - 2\forall_P - \forall_W) \end{aligned} \quad (34)$$

This can be thought of as a second-order extension of the original UD estimate of $\forall_e$ with a correction based on an upwind-biased estimate $(\forall_P - \forall_W)/\delta x$ of the gradient of $\forall$ multiplied by the distance $\delta x/2$ between node P and the east face (Versteeg and Malalasekera 2007).

In TVD scheme, all of the UD, LUD and QUICK schemes are written as follows:

$$\forall_e = \forall_P + \frac{\psi}{2}(\forall_E - \forall_P) \quad (35)$$

It is easy to see that the upwind differencing scheme leads to function $\psi = 0$. But by looking at the other schemes, it can be seen that linear upwind differencing can be rearranges as:

$$\forall_e = \forall_P + \frac{1}{2}\left(\frac{\forall_P - \forall_W}{\forall_E - \forall_P}\right)(\forall_E - \forall_P) \quad (36)$$

where ψ is equal to $\forall_P - \forall_W / \forall_E - \forall_P$ and for QUICK approximation expression, this can be rewritten as:

$$\forall_e = \forall_P + \frac{1}{2}\left(\left(3 + \frac{\forall_P - \forall_W}{\forall_E - \forall_P}\right)\frac{1}{4}\right)(\forall_E - \forall_P) \quad (37)$$

Hence, ψ is equal to $\left(3 + \forall_P - \forall_W / \forall_E - \forall_P\right)\frac{1}{4}$.

According to the Equations 36 and 37, the relations of upwind-side gradient to downwind-side gradient calculate the value of function ψ. Therefore, it can be written as $\psi = \psi(r)$ where

$$r = \frac{\forall_P - \forall_W}{\forall_E - \forall_P} \quad (38)$$

The general form of the east face value $\forall_e$ can be written as

$$\forall_e = \forall_P + \frac{\psi(r)}{2}(\forall_E - \forall_P) \quad (39)$$

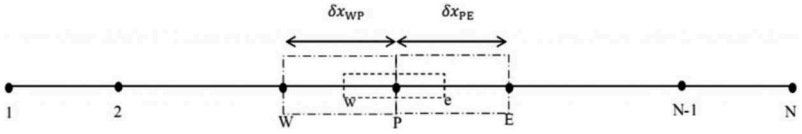

Figure 3. One dimensional discretization of FVM (Gharehbaghi 2017).

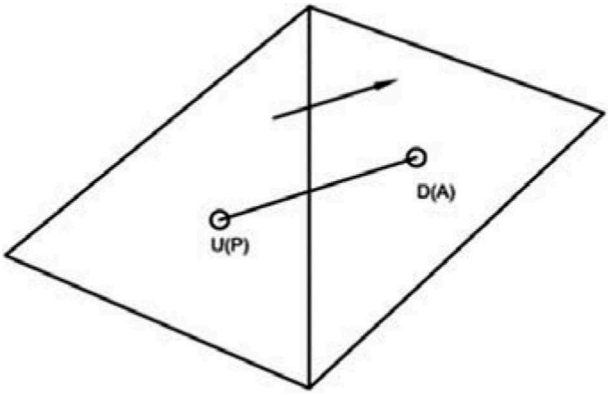

Figure 4. Illustration of node point in unstructured grid system (Gharehbaghi, Kaya, and Saadatnejadgharahassanlou 2017).

In unstructured conditions Equation 39 can be rewritten as follows:

$$\forall_i = \forall_U + \frac{\psi(r)}{2}(\forall_D - \forall_U) \tag{40}$$

where; $\forall_i, \forall_U, \forall_D$ are the values in face of the cell, upstream node point and downstream node point, respectively.

The illustration of node point in unstructured grid system by considering the direction of flow is given in Figure (4). More detail about r in unstructured condition can be found in the Darwish and Moukalled (2003).

6. Solution of governing equations

The final form of the governing equations is presented in this section. All of the equations are solved in explicit conditions. In order to develop the codes, MATLAB software is used.

6.1. Continuity equation

The explicit final form of the continuity equation is given as:

$$(h)^{t+1} = (h)^t - \frac{t}{A}\sum_{m=1}^{M}(L^m)_i\left[(ucos\emptyset + vsin\emptyset)_U h_U + \psi(r)\left((ucos\emptyset + vsin\emptyset)_U h_U - (ucos\emptyset + vsin\emptyset)_D h_D\right)/2\right] \tag{41}$$

6.2. Momentum equation in flow direction (x)

The last configuration of the momentum equation in the flow direction (x-) is obtained as:

$$(u)^{t+1} = \left\{\begin{array}{l} (hu)^t - \frac{\Delta t}{A}\left[\sum_{m=1}^{M}\frac{1}{2}gL^m\begin{pmatrix} h^2{}_U cos\emptyset + \psi(r) \\ ((h^2{}_U cos\emptyset - h^2{}_D cos\emptyset))/2 \end{pmatrix}\right. \\ + \sum_{m=1}^{M} L^m(hu^2cos\emptyset)_U + \psi(r) \\ \left((hu^2cos\emptyset)_U - (hu^2cos\emptyset)_D\right)/2) \\ + \sum_{m=1}^{M} L(huvsin\emptyset)_U + \psi(r) \\ \begin{pmatrix} (huvsin\emptyset)_U - (huvsin\emptyset)_D)/2) \\ -\sum_{m=1}^{M} L^m\left(\frac{h}{\rho}T_{xx}\right)_U + \psi(r)\left(\left(\frac{h}{\rho}T_{xx}\right)_U - \left(\frac{h}{\rho}T_{xx}\right)_D\right)/2 \end{pmatrix} \\ -\sum_{m=1}^{M} L^m\left(\frac{h}{\rho}T_{xx}\right)_U + \psi(r)\begin{pmatrix} \left(\frac{h}{\rho}T_{xx}\right)_U \\ -\left(\frac{h}{\rho}T_{xx}\right)_D \end{pmatrix}/2) \\ \left. -\sum_{m=1}^{M} L^m\left(\frac{h}{\rho}T_{yx}\right)_U + \psi(r)\begin{pmatrix} \left(\frac{h}{\rho}T_{yx}\right)_U \\ -\left(\frac{h}{\rho}T_{yx}\right)_D)/2 \end{pmatrix}\right] + \Delta tS \end{array}\right\}/h^{t+1} \tag{42}$$

6.3. Momentum equation in transect direction (y)

The final form of the momentum equation in the transect direction (y-) is obtained as:

$$(v)^{t+1} = \left\{\begin{array}{l} (hv)^t - \frac{\Delta t}{A}\left[\sum_{m=1}^{M}\frac{1}{2}gL^m(h^2{}_U sin\emptyset + \psi(r)((h^2{}_U sin\emptyset - h^2{}_D sin\emptyset))/2)\right. \\ + \sum_{m=1}^{M} L^m(hv^2sin\emptyset)_U + \psi(r)((hv^2sin\emptyset)_U \\ -(hv^2sin\emptyset)_D)/2) + \sum_{m=1}^{M} L^m(huvcos\emptyset)_U + \psi(r)((huvcos\emptyset)_U \\ -(huvcos\emptyset)_D)/2) - \sum_{m=1}^{M} L^m\left(\frac{h}{\rho}T_{xy}\right)_U + \psi(r)\left(\left(\frac{h}{\rho}T_{xy}\right)_U - \left(\frac{h}{\rho}T_{xy}\right)_D\right)/2) \\ \left. -\sum_{m=1}^{M} L^m(\frac{h}{\rho}T_{yy})_U + \psi(r)\left(\left(\frac{h}{\rho}T_{yy}\right)_U - \left(\frac{h}{\rho}T_{yy}\right)_D\right)/2)\right] + \Delta tS \end{array}\right\}/h^{t+1} \tag{43}$$

6.4. Sediment transport equation

The final form of sediment transport equation is obtained as:

$$(z)^{t+1} = (z)^t - \frac{t}{A}\sum_{m=1}^{M}(L^m)_i\begin{bmatrix} \left(\frac{(ucos\emptyset+vsin\emptyset)}{\sqrt{u^2+v^2}}\right)_U k_s \\ +\psi(r)\begin{pmatrix} \left(\frac{(ucos\emptyset+vsin\emptyset)}{\sqrt{u^2+v^2}}\right)_U k_s \\ -\left(\frac{(ucos\emptyset+vsin\emptyset)}{\sqrt{u^2+v^2}}\right)_D k_s \end{pmatrix}/2 \end{bmatrix} \tag{44}$$

7. Numerical investigations

Two hypothetical cases were employed to examine the numerical results of developed models. In this research, Flow3D software is employed to verify the accuracy and reliability of the proposed model. This software derives rectangular cells to simulate the flow domain. Among the existing turbulence models in

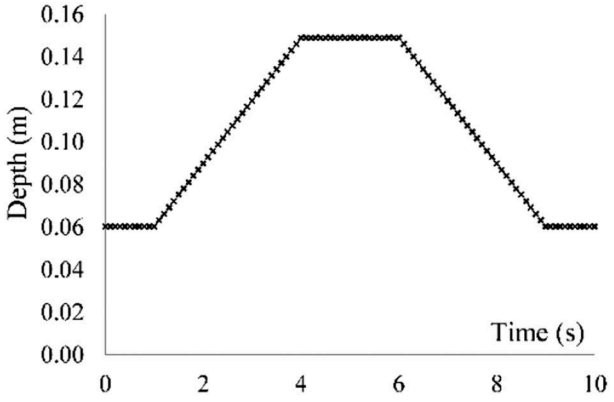

Figure 5. Inlet hydrograph of hypothetical case 1.

the software, Renormaliation Group (RNG) method is employed. The chief difference between RNG model and k-ε model is that equation constants that are calculated empirically in the standard k-ε model are derived explicitly in the RNG model. Additionally, the number of meshes that are used in Flow3D software are 33x201x16 (transect directionx-flow directionxdepth of the flow direction). The calibration of Flow3D software has been done according to the values of the first two authors' study in 2012.

7.1. Hypothetical case 1

In hypothetical case 1, a rectangular channel with 4 m length and 1m width is considered. In the cannel, it is assumed that the thickness of sediment layer is 3 cm. The size and porosity of sediment particles are selected as 0.0032 mm, and 0.5, respectively. The Manning roughness coefficient is chosen as 0.025 for the bed layer and 0.009 for the wall respectively. The channel slopes are assumed to be 0.005 and 0.002 in flow (*x*-) and transect (*y*-) directions, respectively. Note that small value for a particle diameter and a large value for the Manning's coefficient are employed. In an ideal (or real) case, larger sediment particle and lower roughness coefficient could be more realistic. However, since the objective is to test the performances of the models for the same hypothetical cases, the chosen values could not prevent the achievement of this goal.

For the initial conditions, the depth of water is assumed as 0.06 m while the velocities of water in flow (*x*-) and transect (*y*-) directions to be 0.435 m/s and 0 m/s, respectively. For boundary conditions; the hydrograph that is given in Figure (5) is considered as inlet hydrograph. The illustration of comparison between the developed model by the depth-averaged parabolic eddy viscosity model and mixing length model are given in Figures 6–11.

In Figures 6–11, the abbreviations of Flow3D, EVMTVD, MLMTVD stand for the numerical results of depth of water in Flow3D software, depth-averaged parabolic eddy viscosity turbulence model, mixing length turbulence model, respectively. The abbreviations of Flow3DZ, EVMTVDZ MLMTVDZ refers to the results of bed deformation in Flow3D software, depth-averaged parabolic eddy viscosity turbulence model and mixing length turbulence model, respectively. It is worth pointing out that the illustration of water surface profile is just given along the middle of the channel (*x*- direction) while the illustration of bed deformation is given in both of length and width of the channel (*x*- and *y*- directions).

The illustration of water surface profiles and bed variations at 5^{th} and 10^{th} s along the middle of the channel (y = 0.5m) are given in Figure 6–7. According to Figure 6; the depth-averaged parabolic eddy viscosity turbulence model and mixing length turbulence model predict water surface profile with good agreement. Yet, the numerical results of mixing length turbulence model are closer to the numerical results of Flow3D software. As seen, both models also satisfactorily simulate bed profiles, including the scour at the upper part of the cannel.

The numerical results of water surface profile and bed variations by depth-averaged parabolic eddy viscosity turbulence model and mixing length turbulence model against the numerical results of Flow3D software are also satisfactory at the 10^{th} second of the simulation (Figure 7). The mixing length turbulence

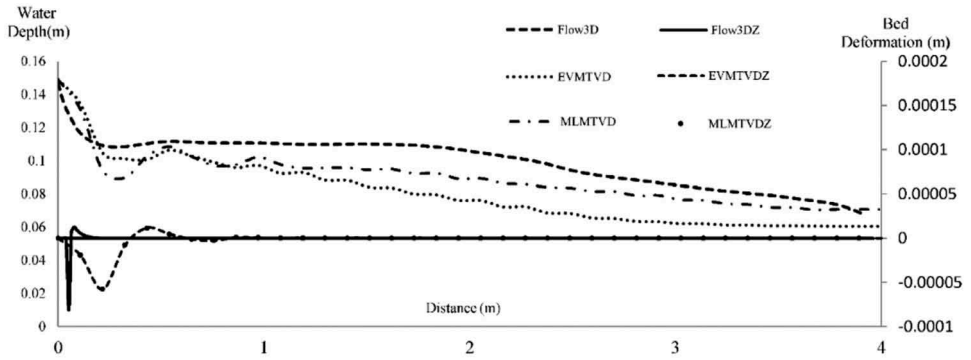

Figure 6. Illustration of water surface profile and bed deformation in flow direction in 5th s (y = 0.5).

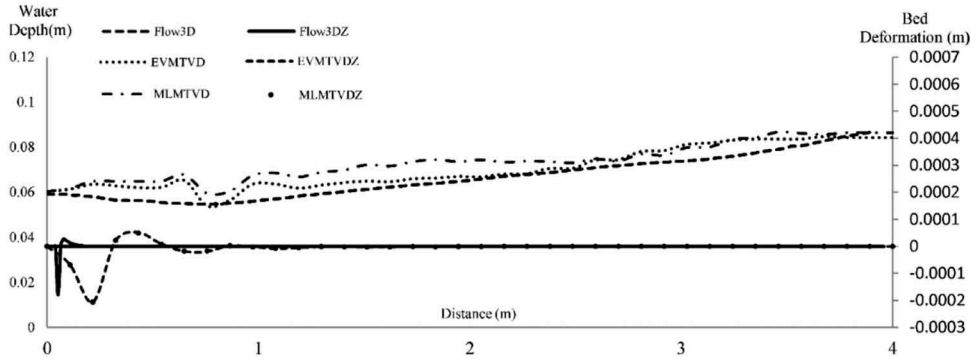

Figure 7. Illustration of water surface profile and bed deformation in flow direction in 10th s (y = 0.5).

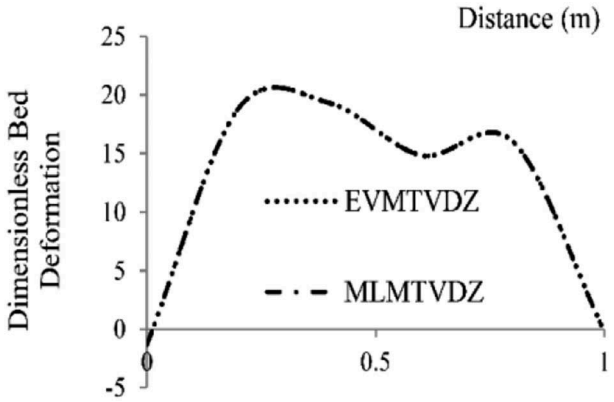

Figure 8. Dimensionless differences between Flow 3D and turbulence models in 1th m and 5th.

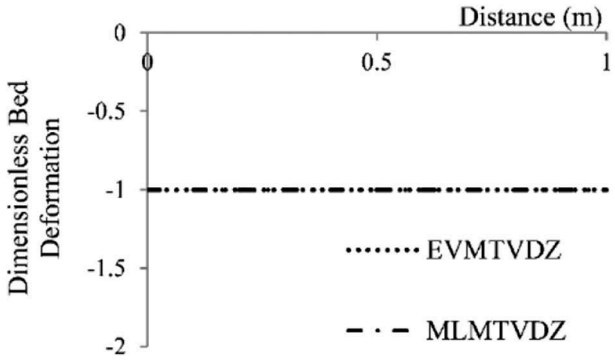

Figure 10. Dimensionless differences between Flow 3D and turbulence models in3th m and in 5th s.

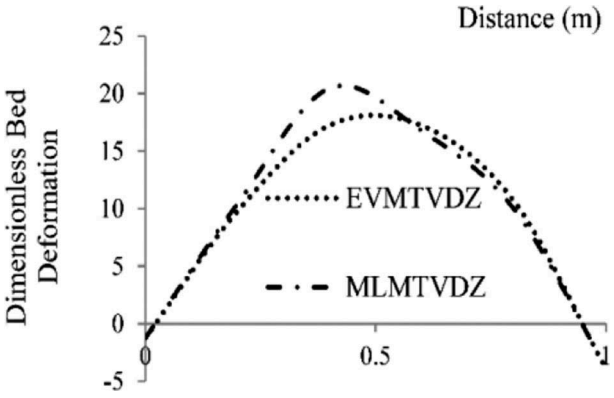

Figure 9. Dimensionless differences between Flow 3D and turbulence models in 1th m and in 10th s.

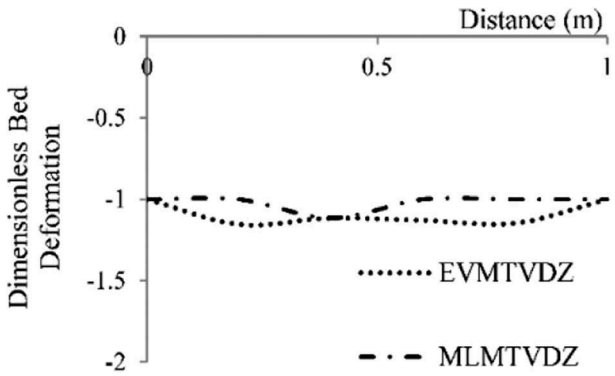

Figure 11. Dimensionless differences between Flow 3D and turbulence models in 3th m and in 10th s.

model shows slightly better results than depth-averaged parabolic eddy viscosity turbulence model.

In order to compare the numerical results of transect bed deformation (y- direction), between depth-averaged parabolic eddy viscosity turbulence model and mixing length turbulence model the dimensionless bed deformation is calculated as:

$$\mathrm{DBD} = (\mathrm{Bdpara} - \mathrm{Bdflow})/\mathrm{Bdflow} \qquad (45)$$

where; DBD = Dimensionless Bed Deformation, Bdpara = Bed deformation of depth-averaged parabolic eddy viscosity turbulence model or mixing length turbulence model, and Bdflow = Bed deformation of Flow3D software.

The illustration of dimensionless bed deformation at the same time and in the two different transect of the channel (x = 1 m and x = 3 m) are given in Figure 8–11. According to these figures, it can be seen clearly that both of the turbulence models could predict bed deformation. The numerical results of mixing length turbulence model are more reliable than the numerical results of depth-averaged parabolic eddy viscosity turbulence model.

7.2. Hypothetical case 2

A channel with 5 m length and 0.8 m width is assumed as hypothetical case for which 3 cm erodible layer with 0.0032 mm diameter and 0.5 porosity of sediment particles are assumed. The required values of manning roughness coefficient for separated sediment, manning roughness coefficient of wall, and slope of the channel in flow direction (x-) and transect direction (y-) are assumed to be 0.04, 0.009, 0.005 and 0.002, respectively. Note that small value for a particle diameter and a large value for the Manning's coefficient are employed. In an ideal (or real) case, larger sediment particle and lower roughness coefficient could be more realistic. However, since the objective is to test the performances of the models for the same hypothetical cases, the chosen values could not prevent the achievement of this goal.

Suspended-sediment load is a key indicator for assessing the effect of land use changes and engineering practices in water courses (24). In this hypothetical case, it is assumed that suspended sediment load has been added in the beginning of the channel to the clear water. The initial and boundary conditions that has been enforced to the channel are given as follows:

Initial water depth conditions: 0.1 m

Initial sediment concentration conditions: 0 kg/m^3

Velocity of water in flow (x-) and transect (y-) directions: 1.044 m/s and 0 m/s

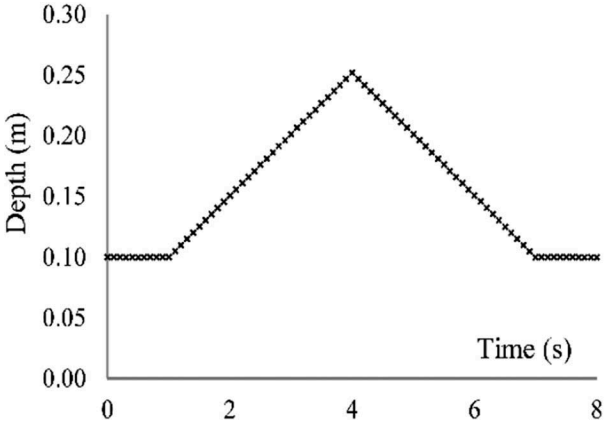

Figure 12. Inlet hydrograph of hypothetical case 2.

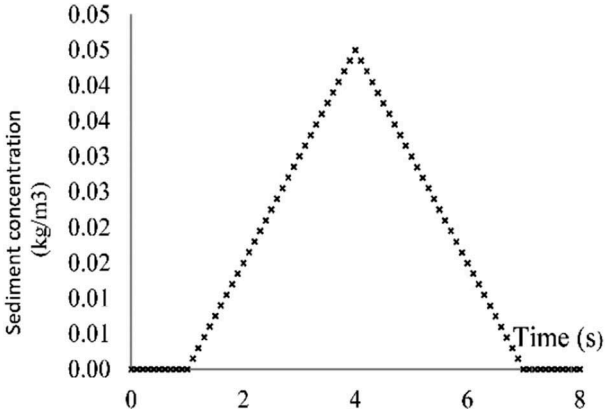

Figure 13. Inlet sediment concentration of hypothetical case 2.

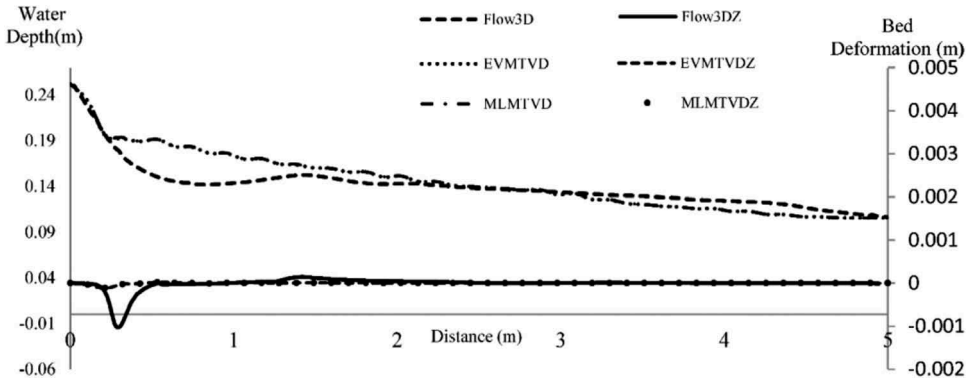

Figure 14. Illustration of water surface profile and bed deformation in flow direction in 4th s (y = 0.4).

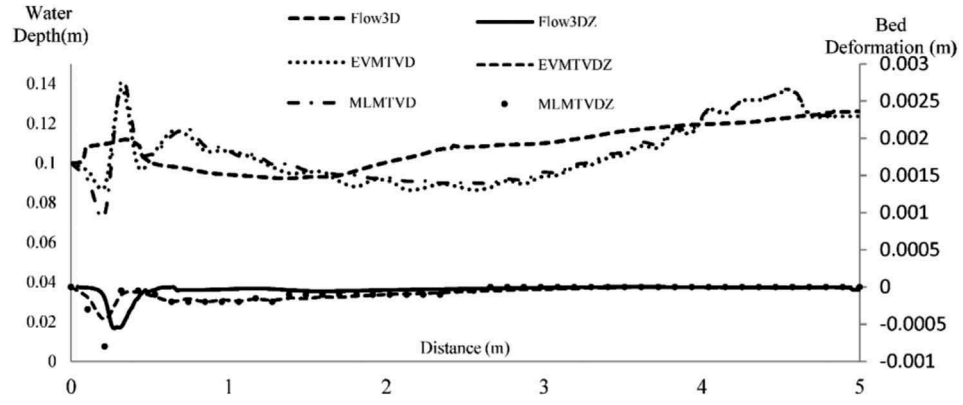

Figure 15. Illustration of water surface profile and bed deformation in flow direction in 8th s (y = 0.4).

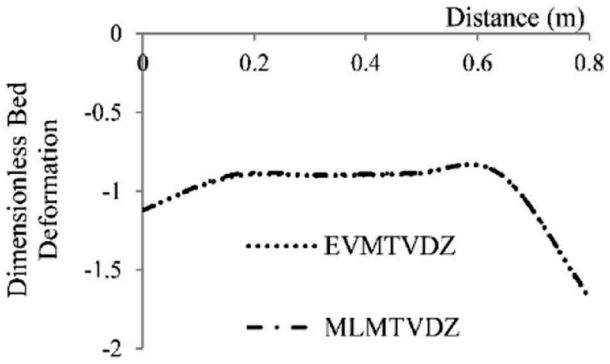

Figure 16. Dimensionless differences between Flow 3D and turbulence models in 2m and in 4th s.

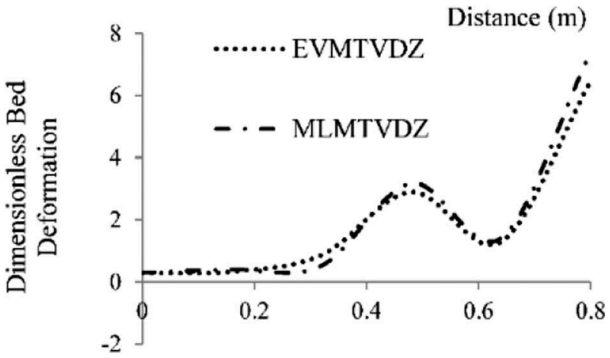

Figure 17. Ddimensionless differences between Flow 3D and turbulence models in 2 m and in 8th s.

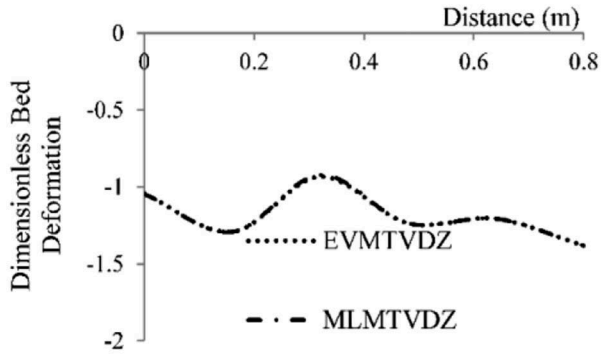

Figure 18. Dimensionless differences between Flow 3D and turbulence models in 4m and in 4th s.

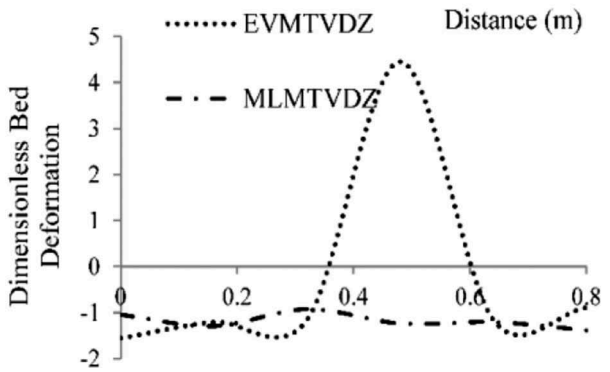

Figure 19. Ddimensionless differences between Flow 3D and turbulence models in 4 m and in 8th s.

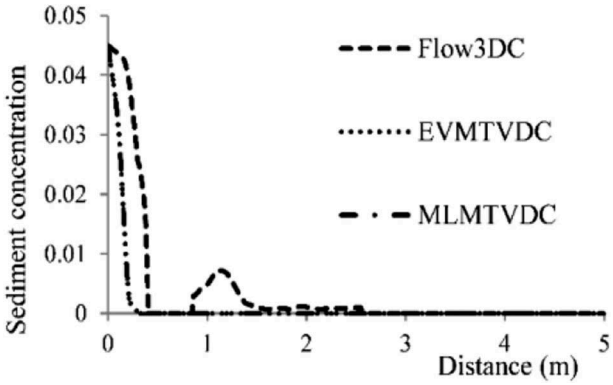

Figure 20. Illustration of sediment concentration in flow direction in 4th s. (y = 0.4).

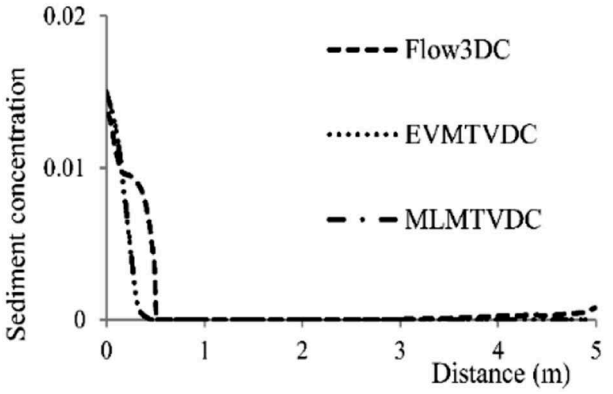

Figure 21. Illustration of sediment concentration in flow direction in 6th s. (y = 0.4).

For boundary conditions; the hydrographs given in Figures (12 and 13) are considered as inlet hydrographs of water and suspended sediment. Moreover, in this hypothetical case, like in hypothetical case 1, the dimensionless bed deformation is calculated by Equation 45.

In Figures 20–21, the abbreviations of Flow3DC, EVMTVDC, MLMTVDC stand for the numerical results of sediment concentration in Flow3D software, depth-averaged parabolic eddy viscosity turbulence model and mixing length turbulence model, respectively.

Figures 14 and 15 are the illustration of water surface profile and bed deformation along the middle of the channel (y = 0.5 m) at 4^{th} and 8^{th} seconds of the simulation period. As seen, both turbulence models could predict water surface profile and bed deformation. The mixing length turbulence model presents slightly better numerical results.

The variation of erodible bed layer along the middle transect of the channel at 4^{th} and 8^{th} seconds are presented in Figures 16–19. Based on these illustrations; although the numerical results of two turbulence models are compatible, the mixing length

turbulence model presents better performance. Figures 20 and 21 present predictions of suspended sediment loads. As seen, the turbulence models could predict suspended-sediment loads satisfactorily.

8. Conclusions

The presented model is composed of two components – hydrodynamic and morphodynamic. The class of TVD schemes is specially formulated to achieve oscillation-free solutions and it is proved to be useful in CFD calculations (Versteeg and Malalasekera 2007). One of the novels of this paper is that the Total Variation Diminishing (TVD) scheme is employed in the simulation of two dimensional bed deformation and suspended sediment load by two turbulence models. The finite volume approach in explicit conditions by TVD scheme is selected to solve the governing equations. In spite of other researchers that employ TVD schemes by Riemann solvers, in this paper this scheme is directly applied to the governing equations. Moreover, the governing equations solved in equilibrium conditions. Two turbulence models, namely the depth-averaged parabolic eddy viscosity turbulence model and the mixing length turbulence model are employed. The numerical results are compared to those of FLOW3D software. Two hypothetical cases were considered for the numerical investigation. In these hypothetical cases; water surface profile, bed deformation and suspended-sediment load were simulated.

Both of the turbulence models could predict water surface bed profiles although the mixing length turbulence model presents better performance. Both models could simulate the scour in the channel as well. Both the models could predict suspended sediment load successfully. It can be concluded that numerical results of mixing length turbulence model are more reliable.

Disclosure statement

No potential conflict of interest was reported by the authors.

Notes on contributors

Dr. Amin GHAREHBAGHI have received his M.Sc. and PhD degrees in Civil Engineering with the particular expertise in Hydraulic Engineering and Water Resources from Dokuz Eylül University in Turkey. During his academic life, he has participated in several experimental and numerical studies and has developed several one and two dimensional numerical models in this field. This author has published several papers and one book in this field.

Prof. Birol KAYA graduated from the Department of Civil Engineering of the Engineering Faculty of Dokuz Eylül University in 1984. He received his master's degree in 1987 and his doctorate degree in 1993 from Dokuz Eylül University, Institute of Science and Technology in Turkey. He currently works at the Dokuz Eylül University. His research interests are in the areas of Computational Fluid Dynamics, Open Channel Hydraulics, and Hydraulics of Pipe Networks.

Prof. Gökmen Tayfur is a faculty member at the Dept. Civil Engineering, Izmir Institute of Technology. He received his B.Sc from the Istanbul Technical University, his M.Sc. and PhD degrees from the University of California at Davis. He has published 80 SCI journal papers, more than 80 conference papers and wrote 2 books and 10 book chapters.

References

Acharya, A. 2011. "Experimental Study and Numerical Simulation of Flow and Sediment Transport Around a Series of Spur Dikes." Ph.D. diss., University of Arizona.

Afshar, H., and S. H. Hoseini. 2013. "Experimental and 3-D Numerical Simulation of Flow over a Rectangular Broad- Crested Weir." *International Journal of Engineering and Advanced Technology (IJEAT)* 2: 6.

Amoudry, L. O., and P. L. F. Liu. 2009. "Two-Dimensional, Two-Phase Granular Sediment Transport Model with Applications to Scouring Downstream of an Apron." *Coastal Engineering* 56: 693–702. doi:10.1016/j.coastaleng.2009.01.006.

Barrios-Piña, H., H. Ramírez-León, C. Rodríguez-Cuevas, and C. Couder-Castañeda. 2014. "Multilayer Numerical Modeling of Flows through Vegetation Using a Mixing-Length Turbulence Model." *Water* 2014 (6): 2084–2103. doi:10.3390/w6072084.

Castro Diaz, M. J., E. D. Fernández-Nieto, A. M. Ferreiro, and C. Parés. 2009. "Two-Dimensional Sediment Transport Models in Shallow Water Equations. A Second Order Finite Volume Approach on Unstructured Meshes." *Computer Methods in Applied Mechanics and Engineering* 198: 2520–2538. doi:10.1016/j.cma.2009.03.001.

Cea, L., and M. E. Vázquez-Cendón. 2012. "Unstructured finite Volume Discretisation of Bed Friction and Convective flux in Solute Transport Models Linked to the Shallow Water Equations." *Journal of Computational Physics* 231: 3317–3339. doi:10.1016/j.jcp.2012.01.007.

Chien, N. 1956. "The Present Status of **Research on Sediment Transport. Trans." *Asce* 121: 833–868.

Darwish, M. S., and F. Moukalled. 2003. "TVD Schemes for Unstructured Grids." *International Journal of Heat and Mass Transfer* 46: 599–611. doi:10.1016/S0017-9310(02)00330-7.

Farsirotou, E. D., J. V. Soulis, and V. D. Dermissis. 2002. "A Numerical Method for 2-D Bed Morphology Calculations." *International Journal of Computational Fluid Dynamics* 16: 187–200. doi:10.1080/10618560290034654.

García-Navarro, P., F. Alcrudo, and J. Savirón. 1992. "1-D Open-Channel Flow Simulation Using TVD-Mccormack Scheme." *Journal of Hydraulic Engineering* 118 (10): 1359–1372. doi:10.1061/(ASCE)0733-9429(1992)118:10(1359).

Gharehbaghi, A. 2017. "Third- and Fifth-Order Finite Volume Schemes for Advection–Diffusion Equation with Variable Coefficients in Semi-Infinite Domain."

Water and Environment Journal 31: 184–193. doi:10.1111/wej.12233.

Gharehbaghi, A., and B. Kaya. 2011. "Simulation of Bed Changes in Rivers with Finite Volume Method by Kinematic Wave Model." *International Journal of Engineering & Applied Sciences (IJEAS)* 3 (3): 33–46.

Gharehbaghi, A., B. Kaya, and H. Saadatnejadgharahassanlou. 2017. "Two Dimensional Bed Variation Models under Non-Equilibrium Conditions in Turbulent Streams." *Arabian Journal of Science and Engineering* 42: 999–1011. doi:10.1007/s13369-016-2258–4.

Kaya, B., and A. Gharehbaghi. 2012. "Modelling of Sediment Transport with Finite Volume Method under Unsteady Conditions." *Journal of the Faculty of Engineering and Architecture of Gazi University* 27: 827–836.

Kaya, B., and A. Gharehbaghi. 2014. "Implicit Solutions of Advection Diffusion Equation by Various Numerical Methods." *Australian Journal of Basic and Applied Sciences* 8: 381–391.

Kuang, C. P., Y. Hang, J. Gu, Y. Pan, and J. Huang. 2011. "A Two-Dimensional Morphological Model Based on a Next Generation Circulation Solver I." *Formulation and Validation" Coastal Engineering* 59: 1–13.

Liu, X., B. J. Landry, and M. H. García. 2008. "Two-Dimensional Scour Simulations Based on Coupled Model of Shallow Water Equations and Sediment Transport on Unstructured Meshes." *Coastal Engineering* 55: 800–810. doi:10.1016/j.coastaleng.2008.02.012.

Meyer-Peter, E., and R. Muller. 1948. "Formulas for Bed Load Transport." *International Association of Hydraulic Research. IAHR* 39–64.

Seo, I. W., I. Jun, and H. S. Choi. 2009. "One-Dimensional Finite Element Model for Suspended Sediment Transport Analysis." *World City Water Forum* 24: 3107–3112.

Tayfur, G., and P. Singh. 2006. "Kinematic Wave Model of Bed Profiles in Alluvial Channels." *Water Resources Research* W06414: 1–13.

Tayfur, G. P., and Singh. 2007. "Kinematic Wave Model for Transient Bed Profiles in Alluvial Channels under Non-Equilibrium Conditions." *Water Resources Research* W12412: 1–11.

V´azquez-Cend´on, M. E., L. Cea, and J. Puertas. 2009. "The Shallow Water Model: The Relevance of Geometry and Turbulence." *Monograf´Ias De La Real Academia De Ciencias De Zaragoza* 31: 217–236.

Vasquez, J., K. Hurtig, and B. Hughes. 2013. "Computational Fluid Dynamics (CFD) Modeling of Run-Of-River Intakes".Hydrovision Conference Proceedings, Denver.

Vasquez, J. A., and B. W. Walsh. 2009. "CFD Simulation of Local Scour in Complex Piers under Tidal Flow" 33rd IAHR Congress: Water Engineering for a Sustainable Environment, Vancouver.

Versteeg, H. K., and W. Malalasekera. 2007. *An Introduction to Computational Fluid Dynamics the Finite Volume Method*. 2th ed. New York: Longman scientific & technical.

Wu, W., D. A. Vieira, and S. S. Y. Wang. 2004. "One-Dimensional Numerical Model for Non-Uniform Sediment Transport under Unsteady Flows in Channel Networks." *Journal of Hydraulic Engineering, ASCE* 130: 914–923. doi:10.1061/(ASCE)0733-9429(2004)130:9(914).

Yafei, J., and S. S. Y. Wang. 2001. "*Two-Dimensional Hydrodynamic and Sediment, Technical Note*," Version 2, Technical Report No. NCCHE-TR-2001-1. Mississippi: University of Mississippi.

Yulistiyanto, B. 2009. "Numerical Modeling on Shallow Water 2D Equations Applied on Flow around a Cylinder." Proceeding of The 6th International Conference on Numerical Analysis in Engineering, Lombok Island, Mataram City.